

This item is likely protected under Title 17 of the U.S. Copyright Law. Unless on a Creative Commons license, for uses protected by Copyright Law, contact the copyright holder or the author.

<https://doi.org/10.1016/j.nima.2006.10.318>

Access to this work was provided by the University of Maryland, Baltimore County (UMBC) ScholarWorks@UMBC digital repository on the Maryland Shared Open Access (MD-SOAR) platform.

Please provide feedback

Please support the ScholarWorks@UMBC repository by emailing scholarworks-group@umbc.edu and telling us what having access to this work means to you and why it's important to you. Thank you.

Extracting first science measurements from the southern detector of the Pierre Auger observatory

L. Wiencke for the Pierre Auger Collaboration

^a*Department of Physics, University of Utah, Salt Lake City, UT 84112, USA*
email: wiencke@cosmic.utah.edu

Abstract

The world's largest cosmic-ray detector is nearing completion in the remote Pampas of Argentina. This instrument measures extensive air-showers with energies from $10^{18} - 10^{20}$ eV and beyond. A surface detector array of area 3000 km^2 records the lateral distribution of charged particles at ground level. A fluorescence detector overlooking the surface detector records the longitudinal light profiles of showers in the atmosphere to make a calorimetric energy measurement. A "test beam" for the fluorescence detector is generated by a calibrated laser near the array center. This talk will focus on detector characterizations essential to the first science results that have been reported from the observatory. Plans to construct a larger instrument in the northern hemisphere will also be outlined.

1. Introduction

The origin of cosmic rays with energies beyond 10^{18} eV is a long standing puzzle. For each decade of energy increase the differential flux falls by three orders of magnitude to approach, at 10^{20} eV, a scant one event per km^2 per century. This alone hints at the formidable instrumental challenges. Fore-runner experiments have operated different types of detectors in different locations. This complicates the understanding of these data in combination because the differing systematics that necessarily underlay astrophysical interpretations can not be compared directly.

The Pierre Auger Observatory combines the surface and air-fluorescence techniques with two co-located detectors. Deployment of the baseline configuration in the south (Fig. 1) is about 75% complete (1100+ of 1600 tanks, 3 of 4 fluorescence "eyes", 3 of 4 LIDARs, 1 of 2 central lasers) and is expected to finish in 2007.

2. Pierre Auger Detectors and their Characterization

The surface detector (SD) (1) of 1600 water cherenkov tanks samples the charged particle lateral distribution of extensive air-showers (EASs) at ground level. With continuous operation and area of 3000 km^2 , the SD provides the statistical engine. After correcting for zenith angle, the density of charged particles 1000 m from the

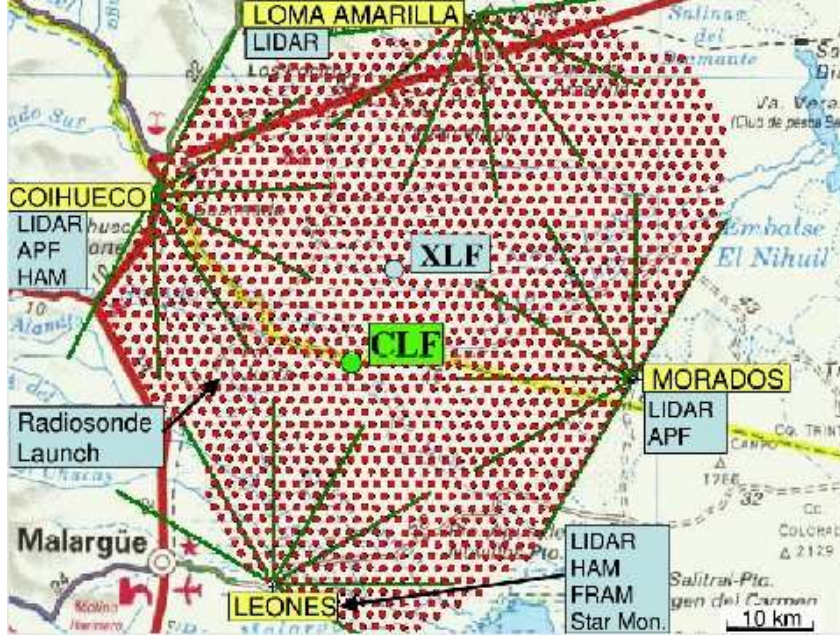


Fig. 1. Configuration of the Pierre Auger Observatory southern detector.(see text.)

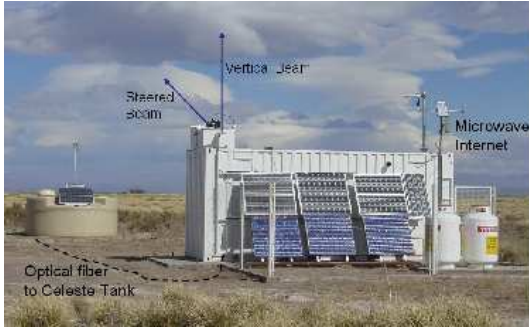


Fig. 2. Central laser facility (CLF) and an adjacent surface detector tank.

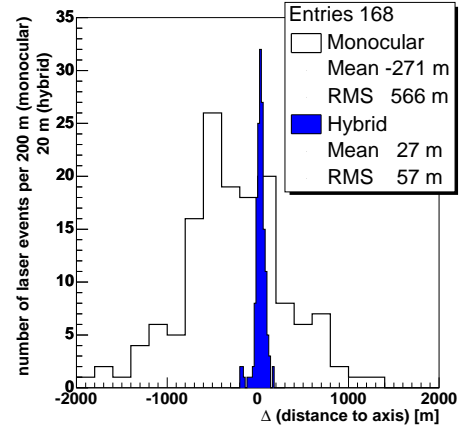


Fig. 3. Rp resolution of CLF vertical tracks as reconstructed using mono (1 FD eye only) and hybrid (1 FD eye + SD timing) data.

shower core provides an energy estimator. For a 10^{19} eV EAS with zenith angle less than 50 degrees, the statistical uncertainty in S1000 is of order 10% (2). Angular accuracy is a function of the number of tanks triggered, which depends primarily on shower energy and zenith angle. For EASs measured by at least 5 tanks, this accuracy is better than 1 degree (3). Essentially all events above 10^{19} eV meet these criteria.

A fluorescence detector (FD) of four “eyes” overlooking the SD operates at night to record the longitudinal light profiles of EASs as they develop through the atmosphere. This calorimetric energy measurement does not rely on interaction models;

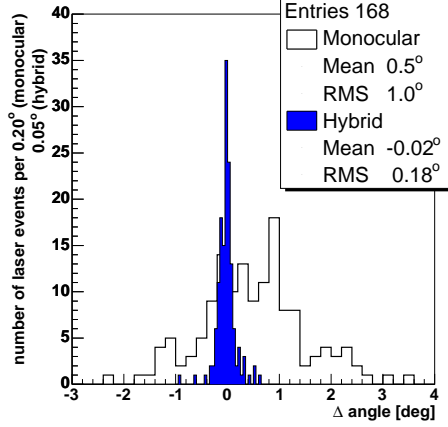


Fig. 4. Angular resolution of CLF vertical tracks as reconstructed using mono (1 FD eye only) and hybrid (1 FD eye + SD timing) data.

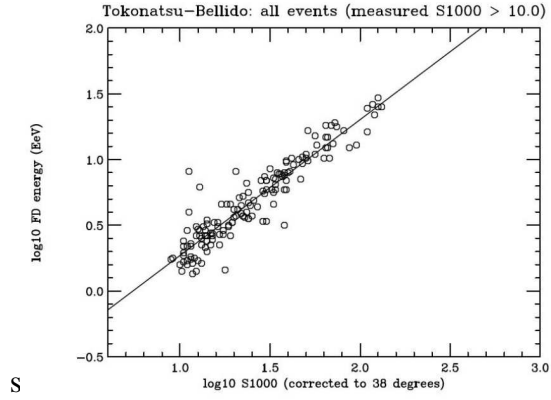


Fig. 5. Energy as measured by the FD (vertical axis) vs s1000 as measured by the SD (horizontal axis).

the amount of fluorescence light emitted is proportional to the energy deposited in the atmosphere. At present the systematic energy uncertainty is less than 25% (Table 1). This value is expected to decrease as improvements are expected in the three largest terms: fluorescence yield, detector photometric calibration, and atmospheric. About 10% of the observed EASs are recorded by both detectors (FD and SD) to construct a “Rosetta stone” hybrid data sample now in excess of 30,000 events.

One important role of the FD, through hybrid data, is to verify the pointing accuracy and to determine the energy scale of the SD (4). To realize this, the Auger design incorporates various methods and instruments to determine the geometrical reconstruction accuracy(5) and the photometric energy scale of the FD(6) and to measure the density profile (7) and the distribution of aerosol in the atmosphere through which the FD observes EASs (8).

Test beams of $E > 10^{17} \text{ eV}$ particles are unavailable. Pulsed UV lasers, however, provide a practical alternative. The total amount of light scattered from a 5 mJ energy UV beam pulse directed vertically into the atmosphere is roughly equivalent to the amount of fluorescence light emitted by a shower with energy in the region of the predicted GZK suppression. The baseline configuration includes two laser facilities, dubbed the CLF (9) (Fig. 2) and the XLF (under construction), near the middle of the SD. The remotely controlled CLF operates during FD data collection to send light simultaneously via optical fiber into a SD tank and via mirrors into the sky. The hybrid laser data sample is used to measure the relative timing between the FD and the SD(10), and to realize significant improvements in geometric reconstruction by invoking the constraint of SD timing (Figs. 3,4). Fitting the longitudinal profile of CLF tracks observed by the FD provides an hourly data base of aerosol optical depth measurements. A comparison between the laser pulse energy and the energy as reconstructed from FD measurements tests, under aerosol-free conditions, the photometric calibration of the FD and the modeling of molecular

	Term	Error(%)		Term	Error(%)
	Light collection	5		Atmosphere (aerosols)	10
	Detector photometric calibration	12		Atmosphere (clouds)	5
	Geometric reconstruction	2		Atmosphere (density profile)	2
	Correction for Missing Energy	3		Fluorescence yield	15
Quadrature Sum = 23					

Table 1

Current estimates of systematic error components to the FD energy measurement.

atmosphere over a total light path of 60 km. The current level of agreement is better than 15%.

Analysis of hybrid EAS data led to many of the first science results. Hybrid events have set the energy scale (Fig. 5) for the first energy spectrum measurement (4), set a limit on the flux of neutral EeV particles pointing back to the galactic center (11), and set limits on the photon fraction of shower composition (12).

3. The Northern Detector and Enhancements in the South

The collaboration has selected southeast Colorado to site the northern detector. Much of this area is accessed by a mile square grid of roads and could support deployment of an array much larger than that in the south. A proposal is in preparation. Enhancement of the southern detector is also anticipated by adding muon counters, in-fill surface detectors and higher elevation angle FD telescopes to reduce the energy threshold towards 10^{17}eV . R&D in radio detection is also planned.

References

- [1] Auger Collaboration, Proc. of 29th ICRC, **7** p1 (2005).
- [2] Auger Collaboration, Proc of 29th ICRC, **7** p167 (2005).
- [3] Auger Collaboration, Proc of 29th ICRC, **7** p17 (2005).
- [4] Auger Collaboration, Proc. of 29th ICRC, **7** p387 (2005).
- [5] Auger Collaboration, Proc of 29th ICRC, **7** p369 (2005).
- [6] P. Bauleo et al., Proc of 29th ICRC, **8** p5 (2005).
- [7] J. Blñer et al., Proc of 29th ICRC, **7** p123 (2005).
- [8] R. Cester et al., Proc of 29th ICRC, **8** p347 (2005).
- [9] A. Arqueros et al., Proc of 29th ICRC, **8** p335 (2005).
- [10] P. Allison et al., Proc of 29th ICRC, **8** p307 (2005).
- [11] Auger Collaboration, Proc of 29th ICRC, **7** p67 (2005).
- [12] Auger Collaboration, Proc. of 29th ICRC, **7** p147 (2005).